EFFECTS OF CALCINATION ENVIRONMENT ON STRUCTURAL AND ELECTROCHEMICAL PERFORMANCE OF $LI_2ZNTI_3O_8$ AS ANODE MATERIAL FOR LITHIUM-ION BATTERIES

A Dissertation Report
Submitted in Partial Fulfilment of the Requirement for the
Award of the Degree
of

MASTER OF SCIENCE

in

CHEMISTRY

by

MANVI (24/MSCCHE/01)

&

KRRISH GUPTA (24/MSCCHE/04)

Under the supervision of

Prof. RAM SINGH & Dr. AMRISH K. PANWAR

Department of Applied Chemistry

DELHI TECHNOLOGICAL UNIVERSITY

(Formerly Delhi College of Engineering)

Shahabad Daulatpur, Main Bawana Road, Delhi- 110042

JUNE 2026

DELHI TECHNOLOGICAL UNIVERSITY

(Formerly Delhi College of Engineering)

Shahabad Daulatpur, Main Bawana Road, Delhi-110042, India

CANDIDATE'S DECLARATION

We, Krrish Gupta(24/MSCCHE/04) and Manvi (24/MSCCHE/O1) students of M.Sc. (Chemistry) hereby declare that the project Dissertation title **"Effects of Calcination Environment On Structural and Electrochemical Performance of $Li_2ZnTi_3O_8$ Electrode Material"** which is submitted by us to the Department of Applied Chemistry, Delhi Technological University, Delhi in the partial fulfilment of the requirement for the award of degree of master of Science, is original and not copied from any source without proper citation. This work has not previously formed the basis for the award of any degree, Diploma, Associateship, Fellowship or other similar title or recognition.

Place: New Delhi

Date: June 2026

Krrish Gupta	**Manvi**
(24/MSCCHE/04)	**(24/MSCCHE/01)**

DELHI TECHNOLOGICAL UNIVERSITY

(Formerly Delhi College of Engineering)

Shahabad Daulatpur, Main Bawana Road, Delhi-110042, India

CERTIFICATE

We hereby certify that the project Dissertation titled **"Effects of calcination Environment on structural and Electrochemical Performance of $Li_2ZnTi_3O_8$ Electrode Material"** which is submitted by Krrish Gupta (24/MSCCHE/O4) and Manvi (24/MSCCHE/01), Department of Applied Chemistry, Delhi Technological University, Delhi in partial fulfilment of the reward of the Master of Science, is a record of the Project work carried out by the student under my supervision. To the best of our knowledge, this work has not been submitted in part or full for any Degree or Diploma to this university or elsewhere.

Place: Delhi

Date: June 2026

Prof. Ram Singh
(Supervisor)

Dr. Amrish K. Panwar
(Co-supervisor)

ACKNOWLEDGEMENT

We would like to express our deepest gratitude to our supervisor, Prof. Ram Singh, Department of Applied Chemistry and Co-supervisor, Dr. Amrish K. Panwar, Department of Applied Physics, Delhi Technological University, Delhi. Their consistent guidance, invaluable suggestions, and ongoing encouragement have helped us complete work. It has been a privilege to work under such kind, motivated, and supportive mentors.

We were fortunate to experience a positive work environment in the laboratory and grateful to all the laboratory staff and research scholars for their cooperation. We are particularly thankful to Mr. Sharad Jadaun and Mr. Satyam Singh for their extensive help in teaching us the fundamentals of various techniques and for his patience in addressing our numerous questions throughout our research. We deeply appreciate all the faculty members of the Departments of Applied Chemistry and Applied Physics at DTU for their continuous support and cooperation. Additionally, we extend our gratitude to both the technical and non-technical staff for their assistance whenever it is needed.

Finally, we would like to express our heartfelt gratitude to our families and friends for their constant encouragement, Support, and motivation throughout this journey. Manvi would also like to convey her sincere appreciation to her friend, Miss Kiran Yadav, for her continuous support, motivation, and encouragement, which greatly contributed to the successful completion of this project.

ABSTRACT

The development of high-performance electrode material with long term structural integrity remains a key stone of advance electrochemical energy storage. $Li_2ZnTi_3O_8$ (LZTO) is a promising anode material due to its structural stability and unique electrochemical properties [1,2]. Despite of its several advantages, its low electrical conductivity is the major challenge in its commercial application. Crystal defects arise from different calcination atmosphere modulates the electronic structure resulting in significant enhancement of the electrical/electrochemical properties of the material. In this study, LZTO has been synthesized via a solid-state method in air and argon environment termed as Air-LZTO and Argon-LZTO respectively. The Structural and Morphological analysis reveals that Argon-LZTO has smaller crystallite size and better morphology in comparison to Air-LZTO due to controlled Argon Environment. The diffusion coefficient calculated from the Warburg coefficient of Ar-LZTO and Air-LZTO is found to be 2.57 x 10^{-15} cm^2s^{-1} and 1.93 x $10^{-15}cm^2s^{-}1$. The Electrochemical Impedance Analysis has employed the Distribution of Relaxation time (DRT) technique to deconvolute the different relaxation processes and understand the overall mechanism. This reveals that the Argon-LZTO has low resistance pathways in comparison to Air-LZTO indicating Better Li^+ ion diffusivity. Cyclic Voltammetry (CV) is used to access the electrochemically active regions and redox peaks. The CV also reveals that Argon-LZTO has better charge capability than Air-LZTO. Overall, Argon-LZTO exhibits superior electrochemical performance than Air-LZTO, indicating that calcination environment affects the structural, morphological, and electrochemical characteristics of the material

CONTENTS

CANDIDATE DECLERATION	2
CERTIFICATE	3
ACKNOELEDGEMENT	4
ABSTRACT	5
CONTENTS	6-8
LIST OF FIGURES	9
LIST OF TABLES	10
ABBREVIATIONS	11
Chapter 1: INTRODUCTION	12
1.1 Rechargeable Batteries	12
1.2 Lithium-ion Batteries	
1.2.1.1 Components of LIBs	
1.2.1.2 Electrolyte	
1.2.1.3 Separator	
1.2.1.4 Anode	
1.3 Principle and Working	
1.3.1 Electrochemistry	
1.3.2 Electrochemical performance	
1.3.2.1 Charge/Discharge	
1.3.2.2 Specific capacitance	
1.3.2.3 Lithium-ion diffusion coefficient	
Chapter 2: Literature Review	
2.1 Types of Anodes	

2.1.1 Transition Metal Oxides	
2.1.2 Mixed Transition Metal oxides	
2.1.2.1 Lithium Zinc Titanate ($Li_2ZnTi_3O_8$)	
Chapter 3: EXPERIMENTAL PROCEDURE	

3.1 Materials and Method	
3.2 Material Characterization	
3.2.1 X- ray diffraction (XRD)	
3.2.2 Scanning Electron Microscopy (SEM)	
3.2.3 Energy dispersive x-ray Spectroscopy (EDS)	
3.3 Electrode Fabrication	
3.4 Electrochemical Measurement	
3.4.1 Electrochemical Impedance Spectroscopy	
3.4.2 Cyclic voltammetry	
Chapter 4: RESULT AND DISCUSSION	
4.1 Structural Analysis	
4.2 Morphological Analysis	
4.3 Electrochemical Analysis	
4.3.1 EIS	
4.3.2 DRT	
4.3.3 CV	
Chapter 5: CONCLUSIONS	
5.1 Conclusion	
5.2 Future Scope	

REFRENCES	
APPENDICES	
Plagiarism Report	

LIST OF FIGURES

Fig.1	Components of lithium-ion Battery
Fig.2	Charging and Discharging of Lithium-ion Battery
Fig.3	Structural Analysis of $Li_2ZnTi_3O_8$, a cubic spinel type material
Fig.4	Schematic representation of synthesis process
Fig.5	Diagrammatic representation of XRD
Fig.6	Diagrammatic representation of SEM
Fig.7	coin-cell assembly representation
Fig.8	XRD Analysis of Calcinated LZTO of Air and Argon
Fig.9	SEM Analysis of LZTO Air and Argon
Fig.10	Elemental Mapping Image Analysis of LZTO (Argon) a) oxygen (green) b) Lithium (Sky blue) c) Zinc (Red) d) Titanium (Yellow)
Fig.11	Elemental Mapping Image Analysis of LZTO (Air) a) oxygen (green) b) Lithium (Sky blue) c) Zinc (Red) d) Titanium (Yellow)
Fig.12	EDS Map Sum Spectrum of LZTO (Air) and Argon
Fig.13	EIS Analysis
Fig.14	Typical DRT profile of a Li-ion cell and the criteria used to evaluate DRT peaks
Fig.15	Cyclic Voltammetry

LIST OF TABLES

Table. 1	Analysis of Cathode Materials
Table.2	Analysis of Anode Materials
Table.3	

ABBREVIATIONS

LIBs	Lithium-ion Battery
LZTO	Lithium Zinc Titanate
TMOs	Transition Metal Oxide
MTMOs	Mixed Transition Metal Oxide
XRD	X-Ray Diffraction
SEM	Scanning Electron Spectroscopy
EDS	Energy Dispersive X-Ray Spectroscopy
EIS	Electrochemical Spectroscopy
CV	Cyclic Voltammetry
DRT	Distribution of Relaxation Time

CHAPTER 1

INTRODUCTION

1.1. Rechargeable Batteries

Energy storage devices which can be charged and discharged many times are called rechargeable batteries or secondary batteries [1]. They are indispensable for many applications, ranging from electrical to energy technology, because of their efficient storage and delivery of electrical energy. The drive for higher energy density, longer cycle operation, safer batteries, and lower cost is the motivation for the development of rechargeable batteries [2-3].

Traditionally, there have been several types of rechargeable batteries:

• **Lithium-Ion Batteries:** The Lithium- ion battery is most used battery in existence and is fundamental to today's electronic gadgets. They are frequently found in mobile phones laptops and many hand-held electronic devices. Compared to most other commercially available rechargeable batteries, lithium-ion batteries are thought to be more advanced due to their higher gravimetric and volumetric energy density. This results in them being able to carry more energy without being heavy and bulky, which is very beneficial for portable electronics and electric vehicles [4].

• **Nickel- Metal Hydrides Batteries:** Nickel–metal hydride (NiMH) batteries are well-established rechargeable batteries that are commonly used in consumer electronics, hybrid and electric vehicles, as well as modern stationary energy storage systems.

They are valued for their reasonable energy/power performance, and because they are safer and more eco-friendly than older battery technologies [5].

Nickel-Cadmium Batteries: Nickel-Cadmium alkaline batteries are the most popular and well-built type of rechargeable batteries utilized for a lot of applications. Main characteristics of Nickel-Cadmium batteries are their high level of cycle stability, long service life and good energy density. They also have a low volume and can be used across a broad temperature range [6].

- **Lead-Acid Batteries:** Widely used Lead-Acid battery, found in automobile, uninterrupted power supply (UPS) systems, telecom backup, and many other energy storage applications. The great popularity of lead –acid batteries is due to their low cost, ease of manufacture, and simplicity of installation. But the limitations are that they have low energy density, shorter cycle life and environmental problem because of using toxic Lead and sulfuric acid [7].

Every rechargeable battery has its own special features, which determine where and how it can be best used.

1.1 Lithium- Ion Batteries:

Lithium-ion Battery (LIBs) are among the most advanced of the rechargeable battery technologies available today. These are popularly used in various application due to their high energy storage and excellent performance [8]. These batteries are popular due to lithium's high electrochemical potential and can move from one electrode material to another while charging and discharging, respectively [9,10].

1.1.1 Components of LIBs

A typical LIB consists of four main components as:

(1) Anode
(2) Cathode
(3) Electrolyte
(4) Separator

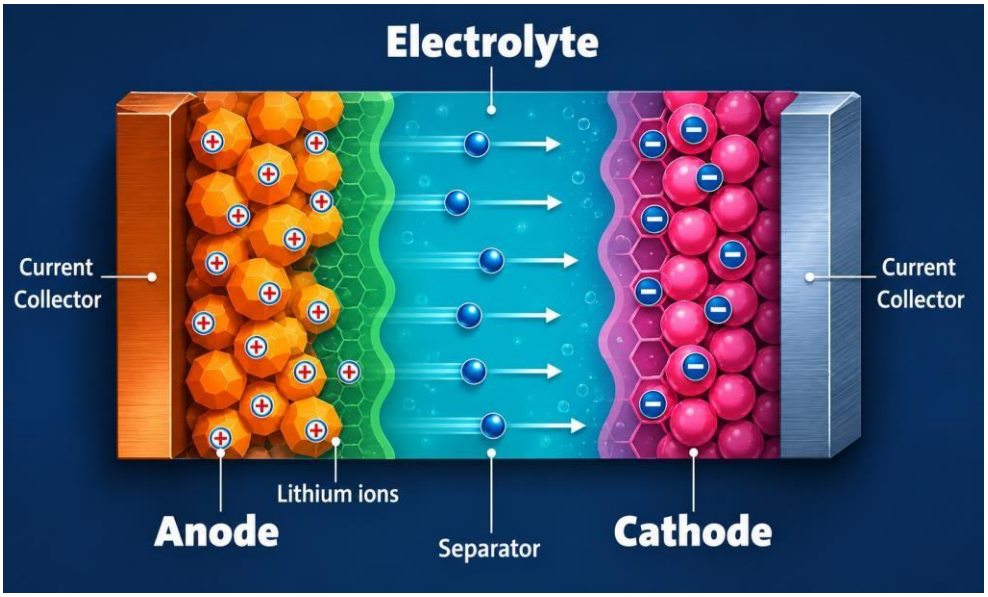


Fig. 1, Components of lithium-ion Battery

1.1.1.1 Cathode

The cathode is a very important part of lithium- ion battery because it affects the battery performance, energy storage capacity, life cycle, and safety. In the Lithium-ion battery, lithium-ion move between the cathode and anode during the charging and discharging, which helps produce electrical energy. Different cathode materials are used depend on battery application [11].

Some of the widely used cathode material in Lithium-ion Battery is:

• **Lithium Cobalt-Oxide ($LiCoO_2$, LCO):** One of the most important cathode materials in lithium-ion batteries, particularly for the portable application, is Lithium Cobalt Oxide (LiCoO2). High energy density and good life cycle make LCO dominant in phones and laptop. The current research interests are directed towards its limitation High-Voltage degradation, side reaction, cost ad sustainability [12].

Vanadium pentoxide (V_2O_5): Among all positive electrode materials (cathodes), vanadium pentoxide (V2O5) is one that is widely studied, with a very high theoretical capacity compared to many commercial materials and has a layered structure. It's research to address its limitations such as poor conductivity and structural instability during battery cycling to realize usage for Li-ion or 'beyond Li' battery applications [13].

• **Nickel Manganese Cobalt Oxide (NMC):** NMC cathodes are widely used in lithium-ion batteries due to their excellent energy storage capacity, safety features, and cost-effectiveness, making them suitable for use in electric vehicles. Nickel improves the battery capacity, manganese enhances the structural stability, and cobalt improves the battery performance and efficiency in these materials. But the costs of cobalt are high and the use of it is environmentally and sustainability questionable. As such, scientists are now turning their attention to designing nickel rich and low and cobalt-free NMC material [14].

• **Lithium Iron Phosphate ($LiFePO_4$):** Lithium Iron Phosphate, known as $LiFePO_4$, is one of the most safe and dependable materials employed in the lithium-ion battery cathode. It is inexpensive, has long durability and stands the test of time to provide an extended battery life, which is ideally suited for eVs and other large scale energy storage systems. Additionally, during battery use it also outputs a stable 3.4 V voltage. Despite that, $LiFePO_4$ does have certain drawbacks such as lower electrical conductivity, slower lithium-ion movement and lower energy density as compared to some other cathode materials [15].

Lithium Manganese oxide ($LiMn_2O_4$): it is relatively low cost and environmentally friendly material in which lithium ions have abundant three-dimensional pathway of diffusion and exhibit very high-rate capability. The material still suffers significant performance when switching on very high voltages or at high temperature, however [16].

Material	Theoretical specific capacity	References
$LiCoO_2$	274 $mAhg^{-1}$	[12]
V_2O_5	437-443 $mAhg^{-1}$	[13]
$LiFePO_4$	170 $mAhg^{-1}$	[15]
$LiMn_2O_4$	148 $mAhg^{-1}$	[16]
$LiNiMnCoO_2$	200 $mAhg^{-1}$	[14]

Table 1: Theoretical Capacity of Cathode Materials

1.1.1.2 Anode

In lithium-ion batteries, the anode act as negative terminal and crucial for storage and removal of lithium- ion during charging and discharging. They can have a significant effect on battery characteristics like energy storage capacity, power performance, battery life and safety. The reactivity of anode is primarily determined by the reaction they undergo with liquid lithium, such as intercalation, alloying and conversion reactions etc. [17].

• **Graphite:** Commercial lithium-ion batteries use the most graphite as the anode material since it is cheap, safe and offers good performance. It has an energy storage

capacity, relatively low volume change in response to lithium intercalation, high corrosion resistance, and is also lightweight, suitable for daily use in batteries [18].

• **Silicon:** Silicon is an interesting alternative to graphite as an anode material for lithium- ion battery due to its ability to hold a considerable amount of lithium, low cost, and its abundance, and environment friendliness. It as high theoretical capacity and energy storage. It suffers from huge volume change during charging and discharging and create a rapid degradation of performance, so stability is big issue for research [19].

• **Lithium Titanate ($Li_4Ti_5O_{12}$):** Lithium titanate (Li4Ti5o12, LTO) is widely used as a safer alternative to graphite as anode material in Lithium-ion battery because of its properties like higher anode voltage led to decrease dendrite formation, zero strain behavior that means no volume change during charging and discharging and fast diffusion coefficient of Li^+ ion makes it suitable for EVs, hybrids, stationary storage [20].

Material	Theoretical capacity	References
Graphite	372 $mAhg^{-1}$	[18]
Silicon	4200 $mAhg^{-1}$	[19]
Lithium Titanate (LTO)	175 $mAhg^{-1}$	[20]
Silicon Oxide (SiO_x)	2200-3580 $mAhg^{-1}$	[21]

Table 2: Theoretical capacity of different anode materials

1.2.1.2 Electrolyte

Electrolytes carry Li+ between anode and cathode and vice versa. Electrolyte strongly control battery safety, power and life cycle. It must possess high ionic conductivity and electric insulation.

•**Organic Electrolyte:** Organic materials are used in electrolytes to help facilitate the movement of lithium ions across battery anodes and cathodes in lithium-ion batteries. Traditionally, ethylene carbonate and dimethyl carbonate organic solvents are made to easily facilitate the dissolution of lithium salts. With the flow of ions, the battery becomes capable of rapid charge/discharge. The ongoing research to help improve battery performance has also considered the development of safer and more stable electrolytes [22].

•**Aqueous Electrolyte:** These aqueous electrolytes consist of highly concentrated salt-water solution that allows the lithium ions to flow between the electrodes and produce energy. Aqueous electrolytes are typically more environmentally friendly and safer than organic electrolytes. Aqueous electrolytes help lithium-ion battery to improve their power and cyclic performance. They can deliver high energy and power density and be utilized in gadgets such as a watch or LED screens [22].

• **Solid state Electrolyte:** Solid state electrolytes play an important role in rapid and safe transport of lithium ion. These electrolytes do not degrade the electrode and do not form the undesirable dendrite which rapid decrease the performance. These properties enhance battery safety, lifespan and performance and contribute to retaining high capacity for many charge cycles [22].

• **Solid Polymer Electrolyte:** Solid polymer electrolytes can transport lithium ions so efficiently at room temperature. These are flexible, have a broad range of temperature for operation and improve battery life and performance. They can work at high voltage, which is desirable for future batteries [22].

• **Gel Polymer Electrolyte:** These are hybrid of solid and liquid electrolyte that improve the performance and safety of lithium-ion battery. They make lithium ions free to move and make stable them at high temperature. These are safer and more reliable for modern batteries as they can absorb liquid electrolytes and decrease the risk of fire [22].

1.2 Principle and Working

During charging and discharging, lithium ions move back and forth between two electrodes in a lithium-ion battery. These ions trapped within the electrode material and are released as require to generate the energy. During normal use, lithium is not converted to metallic lithium, and for this reason the battery is known as a lithium-ion battery [23].

1.2.1 Electrochemistry

When the battery is being discharged (that is, the battery is supplying current), the ions are released from the anode and enter the electrolyte (through the separator) and are deposited in the cathode material. At the same time, electrons are ejected from the anode, travel around the external circuit and fall back into the cathode to maintain the equilibrium of charge [24].

Anode reaction at graphite:

$$Li_xC6 \rightleftharpoons xLi^+ + xe^- + 6 \qquad (1)$$

Cathode reaction of LCO:

$$Li_{1-x}CoO_2 + x\ Li^+ + x\ e^- \rightleftharpoons LiCoO_2 \qquad (2)$$

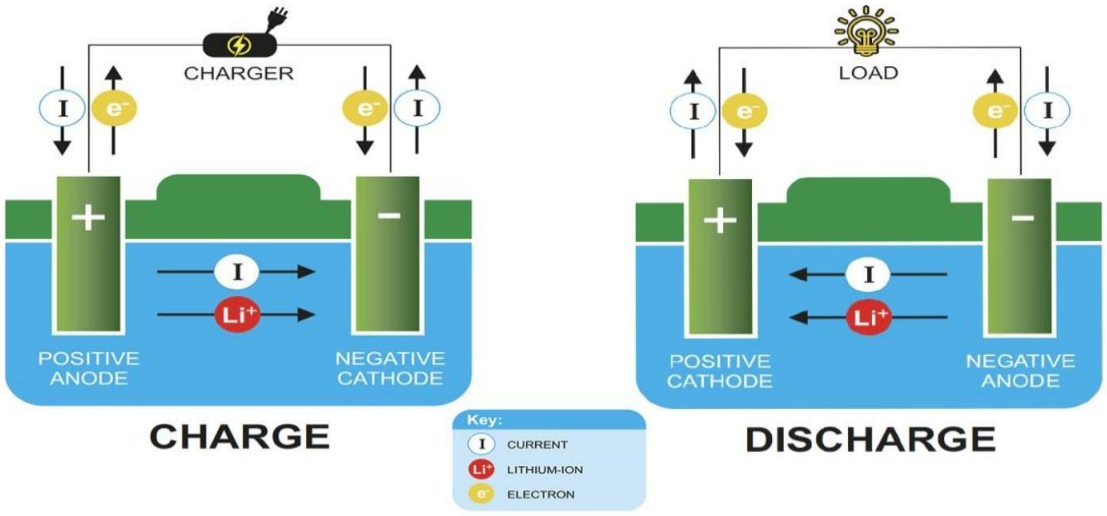


Fig 2: Charging and Discharging of Lithium-ion battery

During charging of lithium-ion battery the ions deintercalated form the cathode, migrate back and intercalate into the anode material. Electrons flow from the cathode through the external circuit to the anode [25].

For a typical LIBs, the average operating voltage is 3.7 V [26]. The overall electrochemical reaction for a LIB can be represented as:

Overall Reaction:

$$Li_xC_6 + Li_{1-x}CoO_2 \rightarrow 6C + LiCoO_2 \qquad (3)$$

1.2.2 Electrochemical Performance

The performance of a LIB is characterized by several key matrices [27]:

1.2.2.1 Charge/Discharge

• **Charge Cycle**: The process of supplying electrical energy to a battery so it can store electrical energy in the form of Chemical energy for later use.

• **Discharge Cycle:** When the battery releases the stored Chemical energy in the form of electrical energy.

• **C-rate:** The rate at which a battery is charged or discharged, as a fraction of its maximum capacity. Slow discharge/charge of a battery (low C-rate) is better for the stability of the electrode material and performance over time. However, if the battery is charged or discharged at a very high C-rate, then it can store and deliver less energy efficiently, which can reduce its overall performance.

1.2.2.2 Specific Capacitance:

Specific capacitance is the measure of the electric charge that can store per unit of mass of a material, expressed in F $g^{-1.}$

Specific capacity is the maximum charge that can be stored by a battery material per gram of that material (mAh g^{-1}). Higher the specific capacity, the higher energy density of battery [29].

1.2.2.3 Lithium-Ion Diffusion Coefficient:

The lithium-ion diffusion coefficient indicates how fast lithium-ions can migrate between electrode and electrolyte. A larger diffusion coefficient shows that the lithium ions freely travel faster, thus allowing the battery to be charged and discharged at different rates. Movement of lithium ions within the electrode is often the slowest step in battery operation and is therefore relatively important to overall performance. This is accomplished by different techniques, including Electrochemical Impedance Spectroscopy (EIS), Cyclic Voltammetry (CV), and Galvanostatic Intermittent Titration Technique (GITT) [30]

CHAPTER 2

LITERATURE REVIEW

This chapter gives a brief overview of the published work on electrode materials for energy storage applications. It primarily covers various anode materials, the electrochemical properties, working mechanisms, and performance of such in lithium-ion batteries.

The chapter also emphasizes the recent developments and key challenges reported by different researchers in this field with regard to research progress.

2.1 Types of Anodes:

The structure and properties of the anode have a significant impact on the performance, efficiency and stability of a rechargeable battery, and are among the most critical components of it [31]. The electrochemical performance improvement methods and strategies of various types of various anode materials are detailed here.

Intercalation-Type Anodes:

The intercalation-type anode materials can store and release energy by the reversible insertion and extraction of lithium ions in and out of the crystal structure of the host material. The lithium-ion batteries which work in this way are called rocking-chair batteries. Graphite is the first practically used anode material having excellent electrochemical characteristics, and it is still in use today due to its structure of layers. When charging, lithium ions enter the interlayer space of the graphite to form LiC_6, which has a low discharge potential< 0.2V(vs Li^+/Li) and is capable of efficiently storing lithium ions [32].

An intercalation-type anode material(M) is described by the following electrochemical reaction. $M + xLi + xe^- \rightarrow Li_xM$

Charging involves the insertion of lithium ion and electron into the crystal structure of the host material (Lithiation). These lithium ions and electrons are released from the structure during discharging, by the process of de-lithiation. This insertion-extraction process is highly reversible with the resulting lattice structure of the battery remaining basically unchanged with repeated charge-discharge cycles, yielding good cycling stability and reliable battery performance.

Alloying-Type Anodes:

Alloy-type anode materials change into alloys with certain metals and semimetals, during charge and discharge. Generally, materials which are used for alloying can be classified into two categories, first one is addition-reaction based materials and the second one is displacement-reaction based materials.

In additional reaction systems the active metal can be used alone or in association with an inactive metal. The volume changes, storage capacity, and operating voltage are the principal ones that are determined by the reaction between the active metal and the lithium/sodium ions. The inactive metal does not directly participate in the alloying reaction, but it can help increase the structural stability and flexibility of the electrode, thus affecting the overall performance of the electrode. Alloy-type anodes have been receiving a lot of attention these days due to their high theoretical capacities, relatively low operating potential (0.1 to 0.8V), and great potential for use in high energy batteries. Displacement or substitution reaction is another reaction pathway in such materials. A binary alloy reacts during the electrochemical process, generating the active metal which binds with the lithium

ions to create lithium rich alloys and help store energy [33].

Conversion-Type Anodes:

In contrast to the traditional intercalation-type materials, conversion-type electrode materials can have much higher theoretical capacities and are typically low cost, making them promise. These materials involve charging and discharging with lithium ions that result in the creation and dissolution of new phases. Theoretical capacities can be up to 1500 or 500mAh g-1, depending on the transition metal compound used to perform the conversion reaction, including oxides, sulfides, fluorides, phosphides and nitrides suitable for this purpose. Transition metal oxides and sulfides have been widely investigated for their high energy storage potential and are considered promising anode materials. Moreover, there are other conversion reactions with lithium and anionic species, which also expand the potential for high-performance electrode materials [34].

$$X + aLi^{+} + ae^{-} \rightleftarrows Li_aX$$

2.1.1 Transition Metal oxides:

The transition metal oxides (TMOs) have been extensively studied conversion-type electrode materials because of their high theoretical capacity and easy handling. In this regard, they have been of great interest to Lithium-ion batteries. Where materials like Fe_2O_3, Co_3O_4, MnO, CuO and NiO have been widely studied. The reversible capacities that have been realized, however, are typically lower than the theoretical values, which is a problem for lithium storage systems. Normally, the voltage corresponding to the reversible capacity of an oxide-based electrode is below 2V. In addition, electrode engineering and adding conductive additives have been demonstrated to increase the reaction kinetics and/or electrochemical performance. The present discussion is to some degree limited to the most

promising oxide-based conversion anodes for lithium-ion batteries [35].

Various parameters including crystal structure, particle size, particle morphology, doping of the electrodes, modifications of the surface, and compatibility with the electrode can highly influence the performance of the TMO electrodes. The control of crystal orientation, reduction of particle size to enhance surface area, engineering of nanocrystalline morphologies, incorporation of heteroatom dopants, and functionalization of the electrode surface with functional groups are all examples of approaches that could lead to improved electrochemical properties.

Transition metal oxides (TMOs) Pros and Cons:

Due to their extremely high theoretical capacities, Cobalt oxides (Co_3O_4, CoO) are widely studied, and are promising candidates for high-energy storage applications. Their practical performance is, however, often hampered by substantial volume changes in repeated charge-discharge cycles, which may result in structural degradation and slow capacity loss over time [36]

Nickel Oxide (NiO) is another material with a high theoretical capacity and with an increasing interest as an anode material. This is an advantage, yet it is undermined by the fact that it experiences significant volume change during cycling, and it does not have a high electrical conductivity, both of which negatively impact cycling stability and rate capability [37]. The low cost, the presence of them in nature, and their environmental friendliness make iron oxides (Fe_2O_3, Fe_3O_4) attractive. However, the repeated volume changes during lithium insertion and extraction can cause moderate cycling stability and degrade the long-term performance [38].

Manganese oxides (MnO_2, Mn_3O_4) have high theoretical capacities and are regarded as environmentally friendly materials. Their application is however restricted due to poor intrinsic electrical conductivity and relatively low-rate capability, which hinders efficient charges of transport and fast electrochemical reactions [39]. In conclusion, the electrochemical properties of the transition metal oxides are promising, but further research is required to fully realize their potential in the development of advanced energy storage systems, and the challenges of volume expansion, structural instability and low electrical conductivity must be overcome.

2.1.2 **Mixed Transition Metal Oxides:**

Mixed transition-metal oxides (MTMOs) are ternary oxides comprising two different metal ions in the same structure instead of being just a mixture of individual metal oxides. Consequently, the material properties have made them an important field of study for a wide range of applications including catalysts, supercapacitors, solar cells, metal-air batteries, and most importantly LIBs.

Recently MTMOs have been considered as potential anode materials for the LIB application due to their several advantages over conventional metal oxides. The synergistic interactions between the two metals is one of their important advantages. The different expansion properties of the metals during charge and discharge of the battery allow for more effective accommodation of the structural changes. For instance, during lithiation, an extra metal oxide structure forms in stannate which results in buffer effects that decrease volume expansion effects and stabilize cycling.

One more major benefit would be their remarkable lithium storage capacity. MTMOs can have reversible capacities greater than many single-metal oxides due to the two electrochemically active metal species that allow them to react with a larger number of lithium ions. Moreover, the electrical conductivity of MTMOs is, in general, also high since the activation of energy for the transfer of electrons between various metal cations is low. This enhanced conductivity promotes faster charge transport and improved electrochemical performance.

MTMOs have also been shown to have environmental advantages and are also seemingly a more sustainable alternative to some of the traditional metal oxide materials. Consequently, considerable research has gone into the design of MTMOs, as well as their composites, as enhanced anode materials for LIBs.

While several studies have been conducted in this field, there are still very few detailed reviews that address the topic of MTMOs for lithium-ion battery applications. Thus, the knowledge of their lithium- storage mechanisms, synthesis methods, structural engineering approaches, and performance enhancement strategies is critical to their potential for going to market as quickly as possible. Special emphasis has been laid on stannate and spinel type materials that have shown great potential as promising next generation anodes for high-performance lithium-ion batteries [40].

Lithium Zinc Titanate ($Li_2ZnTi_3O_8$):

$Li_2ZnTi_3O_8$ possesses a cubic spinel structure with a $P4_332$ space group that is widely used as an active anode material due to its zero-strain property. LZTO has emerged as a promising candidate because of its stable crystal structure, low volume change during cycling, and favorable lithium-ion diffusion characteristics.

Structure:

A cubic spinel structure of LZTO in which oxygen atoms form a close-packed framework, while lithium (Li^+) ions are located mainly at tetrahedral (8a) position, Titanium (Ti^{4+}) ions occupy the octahedral (16d) positions and Zinc (Zn^{2+}) ions also occupy tetrahedral position according to the cation distribution in LZTO.

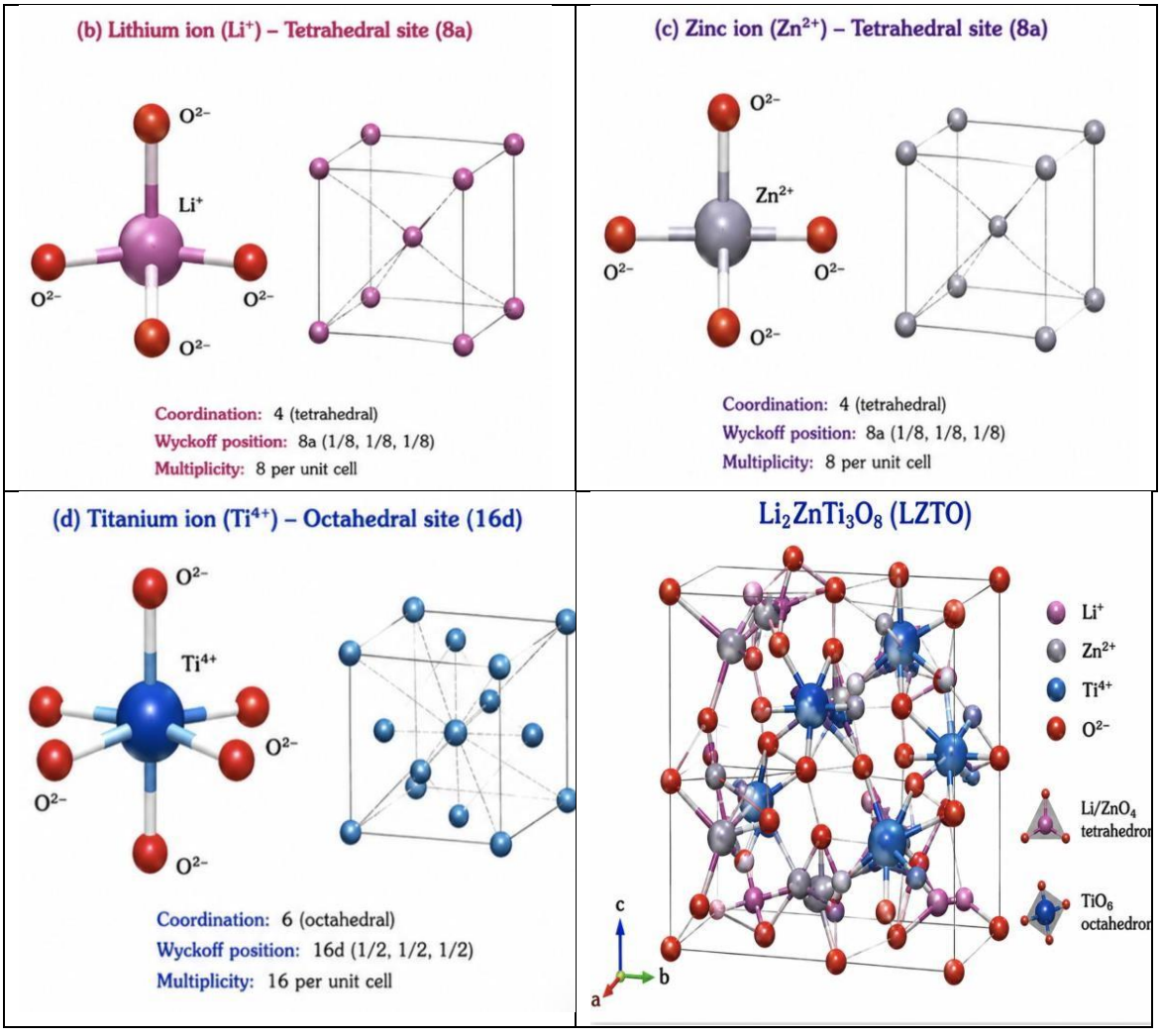


Fig. 3: Structural analysis of LZTO

Lithium-storage mechanism:

The mechanism of lithium storage in LZTO is mainly an intercalation (insertion) reaction as compared to the transition-metal oxides like Fe_2O_3, Co_3O_4, $NiMn_2O_4$ which follow conversion reaction. In the lithiation process, lithium ions are reversibly trapped in the empty lattice place of the spinel, and electrons are transferred through the external circuit.

The overall electrochemical reaction represented as:

$$Li_2ZnTi_3O_8 + xLi^+ + xe^- \rightarrow Li_{(2+x)}ZnTi_3O_8$$

Where x represents the number of inserted lithium ions.

The charge compensation primarily occurs through the reversible reduction and oxidation of Titanium.

$$Ti^{4+} + e^- \rightleftarrows Ti^{3+}$$

Thus, the Ti^{4+}/Ti^{3+} redox couple is mainly responsible for lithium storage. On the other hand, Zn^{2+} mostly serves as a structural stabilizer, and its contribution to a reversible redox process in the normal voltage range is usually small. The host framework remains intact during lithium insertion/extraction process, which causes relatively small volume change, resulting in very high cycling stability and less pulverization of the electrode

CHAPTER 3

EXPERIMENTAL PROCEDURE

This chapter gives an outline of the materials utilized for synthesizing Li_2ZnTi_3O8 in the Air and Argon environment as anode material and fabricating Lithium-half cell for LIBs. It covers all structural, morphological, and electrochemical analysis for the characterization of the electrode material and fabricated electrode.

3.1 Material Synthesis:

The preparation of $Li_2ZnTi_3O_8$ was carried out by a solid-state route via a ball milling method. In analytical, grade Li_2Co_3, Zn $(CH_3COOH)_2$. $2H_2O$, TiO_2, used as a precursor to generate. All the precursors were ball milled in a stoichiometric quantity for the 12h mixing method. Another 5% of lithium source is further added to compensate for the loss of lithium due to its evaporation at high temperature. Dried material that was obtained was ground and then heated at 700°c for 3 hours. Again, treated at 800°c for another 5h in two different environments separately Air and Argon. Finally, the calcinated material reground and use for further electrode preparation and characterization.

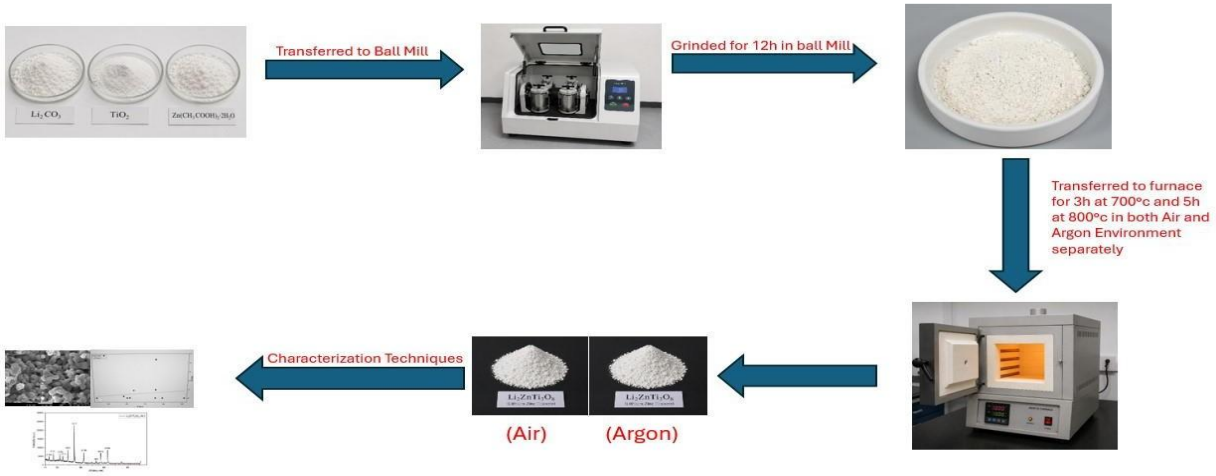


Fig. 4: Schematic representation of synthesis process

3.1. Material Characterization:

All the calcined samples were analyzed using the Rigaku ultimate IV – powder X-ray Diffractometer to study the crystal structure. The measurement is carried out in 2θ range of 10° to 90° using CuKα radiation with a wavelength of 0.154nm. For morphological studies we have done Scanning electron spectroscopy. Electrochemical tests are performed at room temperature on a biological science instruments VMP 3 work station. Cyclic Voltammetry was performed at a scan rate of $0.05mVs^{-1}$. The Electrochemical Impedance Spectroscopy (EIS) technique was used to analyze the electrical response in the frequency range 0f 100KHz to 10mHz under an AC signal.

3.1.1 X- ray Diffraction (XRD):

X-ray Diffractometer (XRD) is an analytical method that is widely used to investigate the crystal structure of materials. It can determine the presence of phases in the materials and give information about the structural properties. The method is based on diffraction effect, where a monochromatic X-ray are diffracted by the periodic arrangement of the atom in a crystal. At a certain angle of incidence, X-ray reflect from the crystal planes in such a manner that constructive interference occurs according to Bragg's law:

$$n\lambda = 2d\sin\theta \qquad (1)$$

Where n = order of diffraction, λ is wavelength of Xray's, d is the distance between the plane of the crystal and θ is the angle of diffraction.

The procedure of a typical XRD experiment is as follows: X-rays are typically produced with a CuKα source and aimed at the sample. The sample is set on the goniometer, which allows the control of the incident angle and the detection angle in an accurate manner. The sample rotates and different crystals planes satisfy the conditions of Bragg's Law and result in diffraction peaks at different angles. Using these peaks, XRD can be used to identify the crystal phase present, calculate the lattice parameters and estimate the crystallite Size of the material.

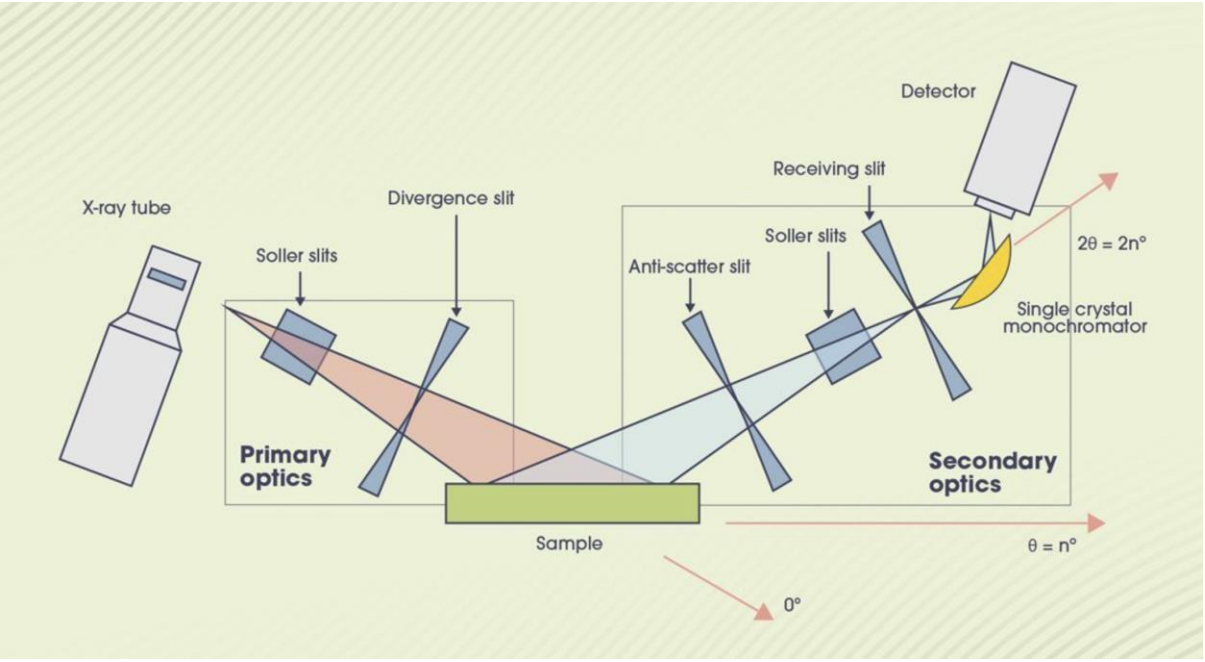


Fig. 5: Diagrammatic representation of XRD

3.1.2 Scanning Electron Microscopy (SEM):

The Scanning Electron Microscopy (SEM) is a very useful imaging tool that allows you to image the surface of materials at high magnifications, from micrometer to nanometer scale. A narrow beam of electrons is focused on a sample surface in SEM. These electrons then interact with the material and subsequently emit different types of signals. Commonly used signals include secondary electrons (SEs) and backscattered electrons (BSEs). These are secondary electrons emerging from the surface of the sample that provide a very high-resolution image of its shape and texture. Backscattered electrons bounce off the specimen, contributing to contrast with heavier elements appearing brighter than lighter ones. It is usually used for observing surface morphology including particle sizes, grain structures, grain boundaries, and surface textures. It is essential in characterization for imaging features of the materials having very high resolution.

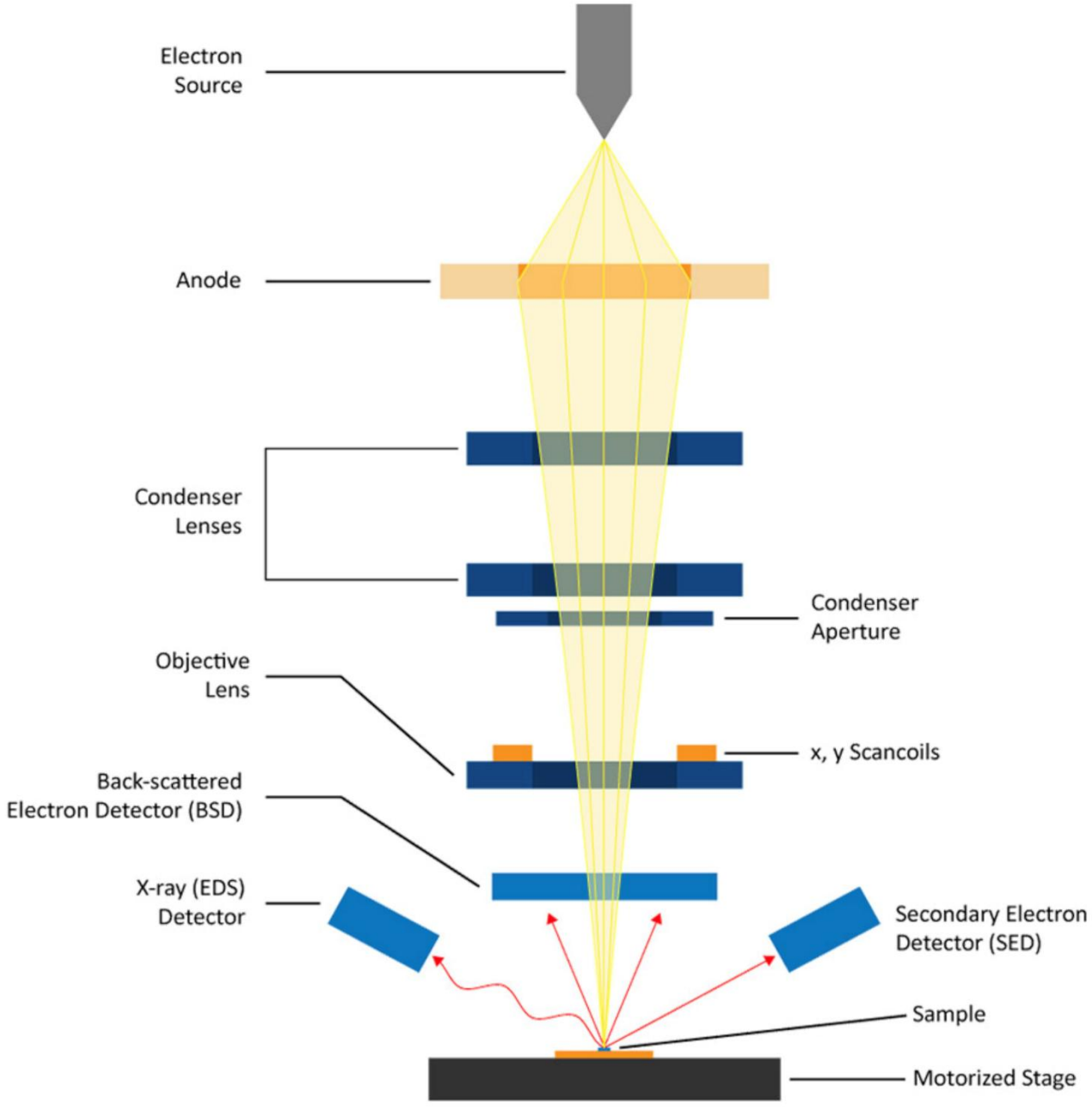


Fig.6: Diagrammatic representation of SEM

3.1.3 Energy Dispersive X-ray Spectroscopy (EDS):

Energy Dispersive X-ray Spectroscopy (EDS) is a technique to identify the elements in a product and quantify the elemental composition of that product. It is typically attached to a Scanning Electron Microscope (SEM) and allows you to perform imaging and elemental analysis on one specimen at a time. The EDS working principle is based on X-ray emission at a specific energy source from an atom that has been collimated by high-energy electrons. When it collides with the electron beam, the electron can be emitted from the inner shell of an atom to leave a vacancy. This vacancy is then occupied by an electron of a higher energy level. An X-ray is emitted during this process. Each X-ray possesses a different energy, enabling the signals that are generated to identify the elements making up the sample. EDS may provide qualitative and semi-quantitative data for the elemental composition of a sample. Use it frequently used the identification of elements in a sample and their relative abundance of quantification across multiple areas within a sample.

3.2 Electrode fabrication:

The slurry was prepared using the active material, super p, and polyvinylidene fluoride (PVDF) binder in the ratio of 80:10:10 in N- methyl pyrrolidone (NMP) solvent and stirred over night until viscus liquid is formed. Then the slurry was spread on a copper current collector using Doctors blade and dried over night at 120°C. Further were punched using 16mm die and transferred inside the Mbraun Glovebox. The Lithium Half cells were fabricated in CR2032 coin cell case where as prepared LZTO electrode used as a working electrode, lithium metal as a reference electrode, Celgrad 2400 polypropylene film used as a separator material to prevent short circuiting and LiPF6 used as an electrolyte.

The coin cell is crimped after assembly using a crimping machine to seal the coin cell. The fabricated coin - cell was transferred outside the glovebox and connected with VMP-3 Biologics potentiostat for further electrochemical characterization.

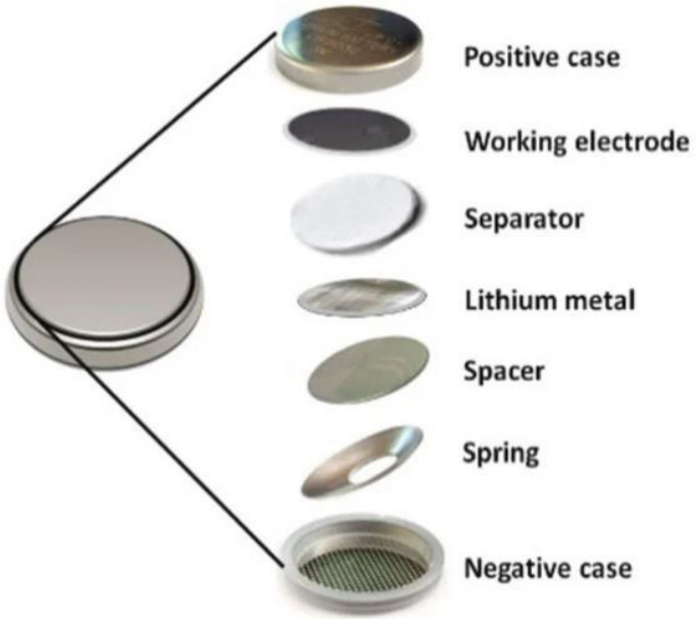


Fig. 7: Coin cell- assembly representation

3.1 Electrochemical Measurement:

There are many electrochemical techniques that have been used to explore the electrochemical behavior and performance of materials. They are based on the interaction between electrical energy and chemical reactions allowing the study of reaction kinetics, charge transfer, and energy storage properties. Two electrochemical methods were used in this work. Electrochemical Impedance Spectroscopy (EIS) and Cyclic Voltammetry (CV). These measurements have been performed with Biological potentiostat and software EC-Lab.

3.1.1 Electrochemical Impedance spectroscopy:

EIS is a technique employed to investigate the electrical and electrochemical response of electrode material. It works by applying a small AC signal over a wide range of frequencies and measuring the impedance response of the system. The obtained data are usually represented as Nyquist plot, which provides information about the solution resistance (Rs), charge transfer resistance (Rct), and lithium-ion diffusion (Warburg impedance). Lower Rct value is better for charge transfer and has better electrochemical kinetics. Hence, EIS has become a main technique for characterizing the conductivity, the interfacial properties, and the performance of lithium-ion battery material.

3.1.2. Cyclic Voltammetry:

Cyclic Voltammetry (CV) is a widely used electrochemical technique for studying the redox behavior and reaction kinetics of electrode materials. In this method, the electrode potential is swept linearly between two predetermined limits and then reversed at a fixed scan rate while the resulting current is recorded. The obtained current–potential (I–V) curve, called a cyclic voltammogram, provides information about oxidation and reduction processes. The positions of the anodic and cathodic peaks indicate the redox potentials, while the peak currents reflect the electrochemical activity of the material. CV also helps evaluate the reversibility of lithium-ion insertion/extraction, charge storage mechanism, and electrode stability. Therefore, it is an essential technique for assessing the electrochemical performance of lithium-ion battery materials.

Chapter 4
Result &Discussion

4.1 Structural Analysis:

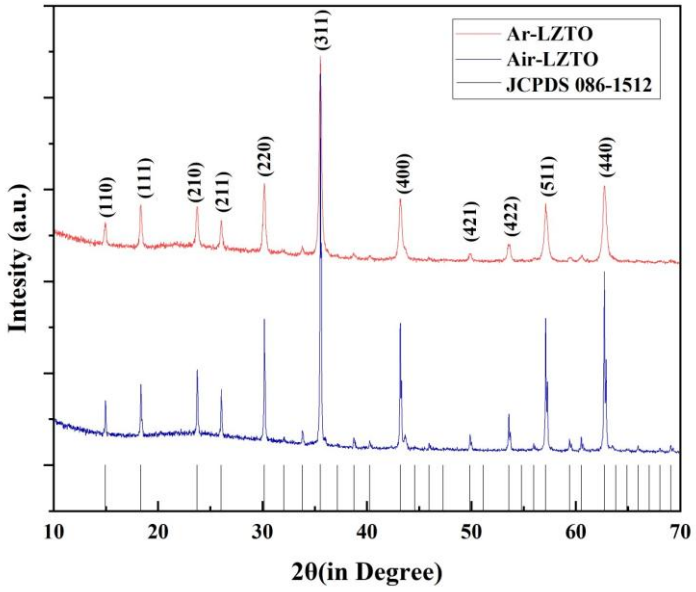


Fig. 8: X-ray analysis of LZTO in Air and Argon Environment

XRD analysis was carried out to confirm the formation of crystalline nature of the synthesized LZTO samples. Figure shows the XRD pattern of $Li_2ZnTi_3O_8$ (LZTO) of Air and Argon along with JCPDS file signifying the formation of cubic spinel crystal structure of LZTO conforming the space group P4332. All the diffraction peaks are very sharp and indicating the crystalline nature of both samples. By the help of Scherrer's formula, the average crystallite size of the sample is calculated as mentioned below:

$$D = \frac{k\lambda}{\beta cos\theta}$$

Where D, λ, K and β are the size of crystalline in nm, wavelength of X-ray (around~0.154nm), shape constant (~0.94), grazing angle in degree, and FWHM corresponding to θ in radian respectively.

The average crystallite Size of Ar-LZTO and Air-LZTO is found to be 29.88nm and 56.70nm respectively. The decrease in average crystallite size in Argon environment with respect to air

environment can be attributed to controlled grain growth. The reduced crystallite size might shorten Li-diffusion path enhancing overall electrochemical performance.

4.1 Morphological analysis:

The SEM image of the calcined pristine LZTO(Air) and LZTO(Argon) samples are presented in figures. Both samples show a prism – like shape, and the appear clustered together, as analyzed by image j software. The average particle size value of Air and Argon is 180nm and

154.7nm respectively. The reduction in the particle is due to controlled environment. In the air environment, there is abundance of oxygen resulting particles to grow and agglomerate in a significantly larger extent 180nm in a high lattice diffusion rate and high migration rate of grain boundaries. However, in controlled Argon environment, there is limited supply of oxygen leading to reduce grain growth and lower aggregate grain size, more uniform, and less agglomerated nanoparticle. the electrochemical properties of LZTO as an anode material will be significantly improved with a small particle size obtained under the argon atmosphere. Due to decrease in the particle size from 180nm to 154.7nm, it drastically shortens the diffusion path length (L) of Li^+ ions. This rapidly increase insertion/de-insertion kinetic rate, also smaller particle size, High surface area and high pore volume means the density of active site is high, which might enhance its electrochemical performance [41].

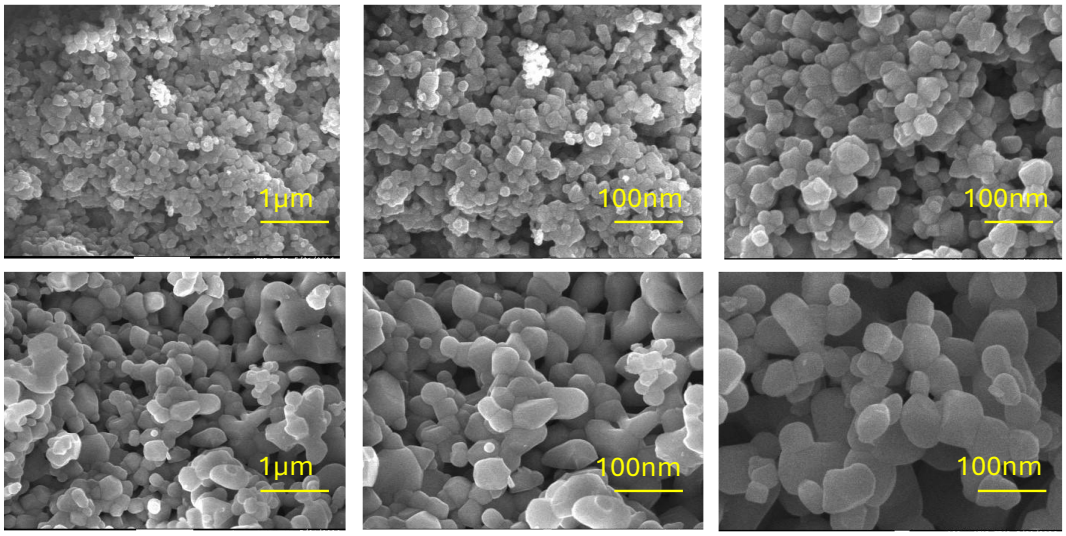


Fig. 9: SEM Analysis of LZTO (Ar) and LZTO (Air)

4.1 EDS Analysis:

The EDS spectra of both air and argon – synthesized LZTO samples shows characteristic peaks of O, Ti, Zn, and Li which indicate the formation of the Target phase of $Li_2ZnTi_3O_8$. There was no peak observed corresponding to any impurities, suggesting high chemical purity of the synthesized materials. Slight difference in peak intensity is observed but are due to different measure conditions and different region analyzed rather than compositional variation. Elemental mapping analysis indicate that the sample prepared under the argon atmosphere has a more uniform distribution of Zn, Ti, and other than air treated sample, The Air sample has noticeable Zn- rich agglomerations of particles and heterogeneous in distribution with the low porosity while the argon one has no Zn agglomerations and homogeneous distribution of particle with better porosity.

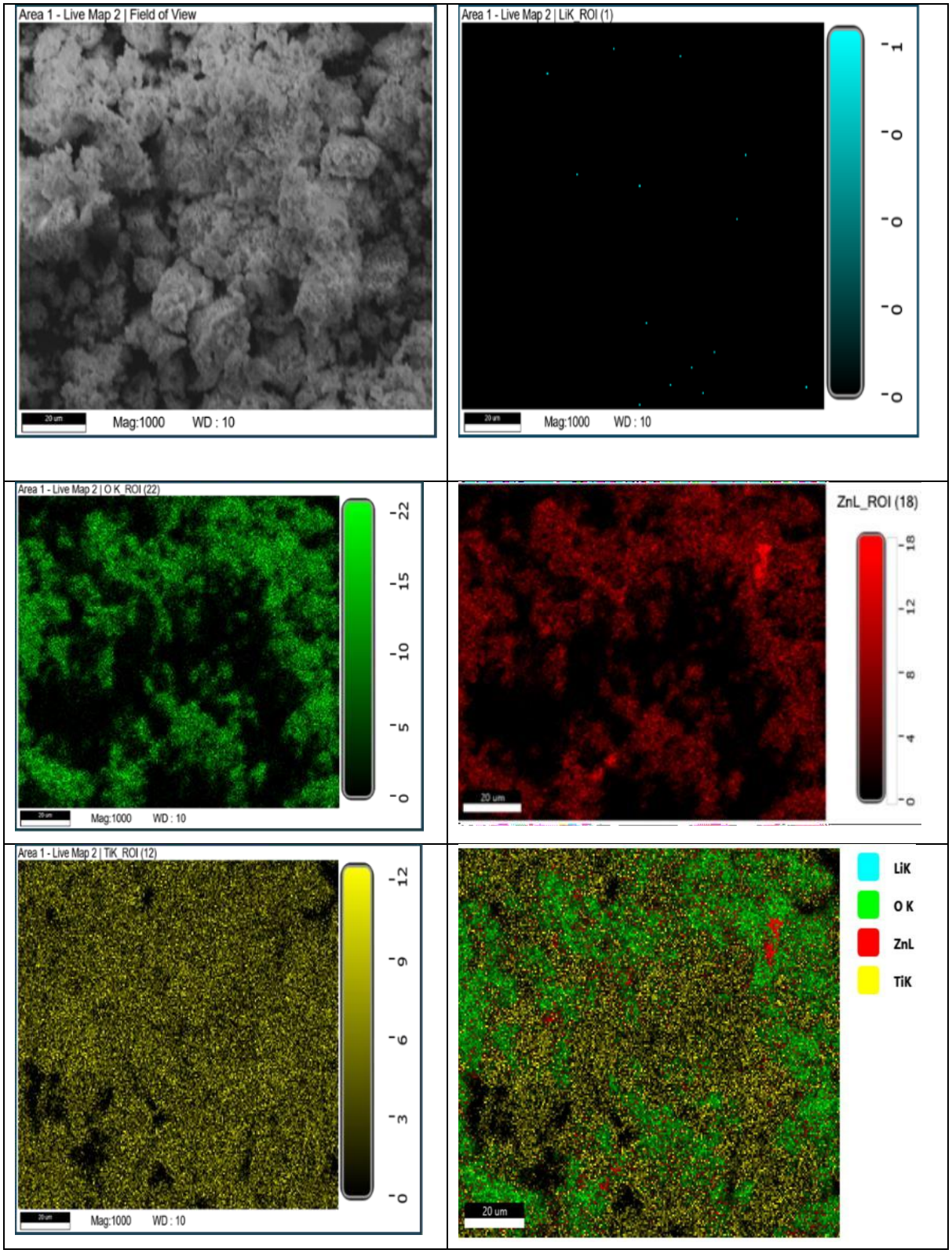


Fig. 10: EDS Images of LZTO (Ar)

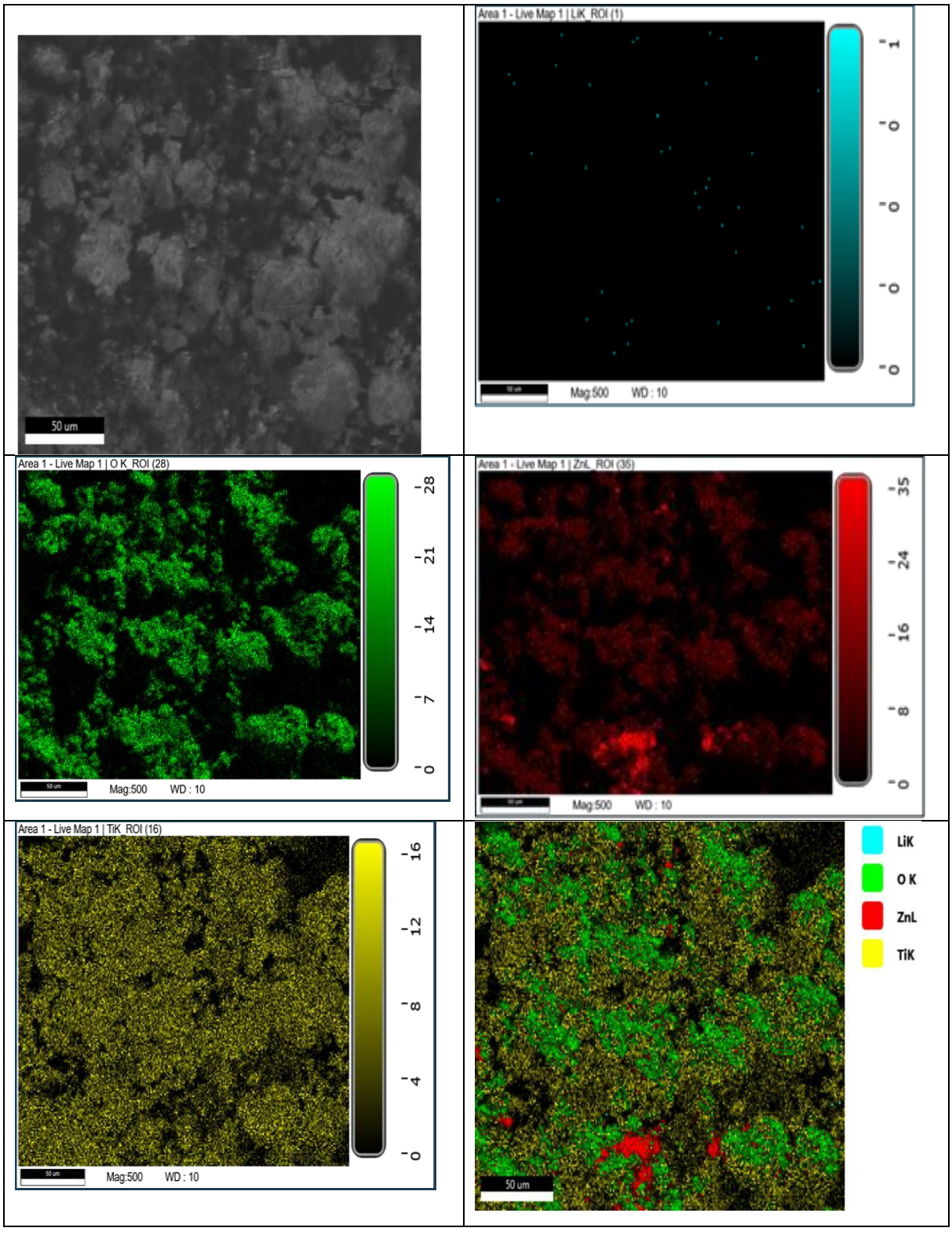
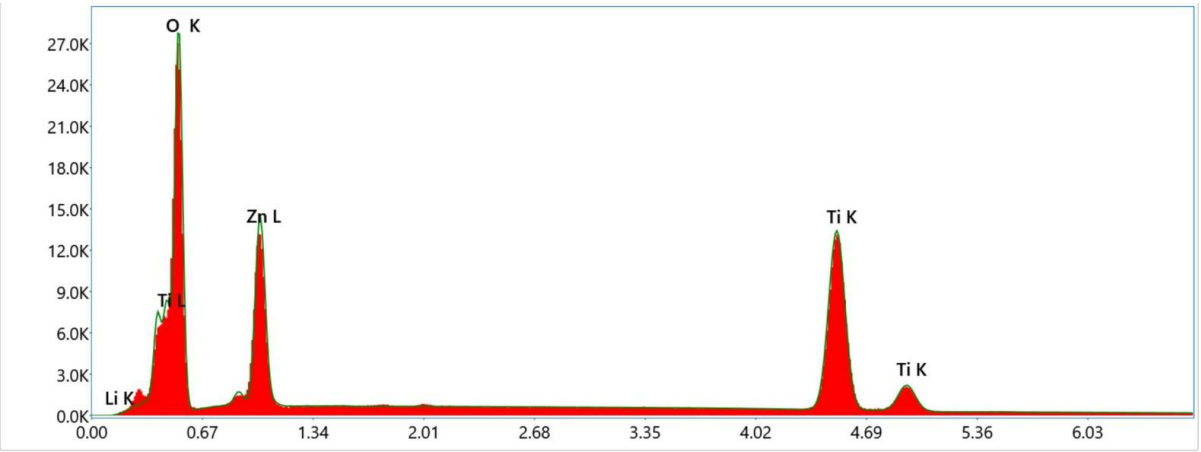
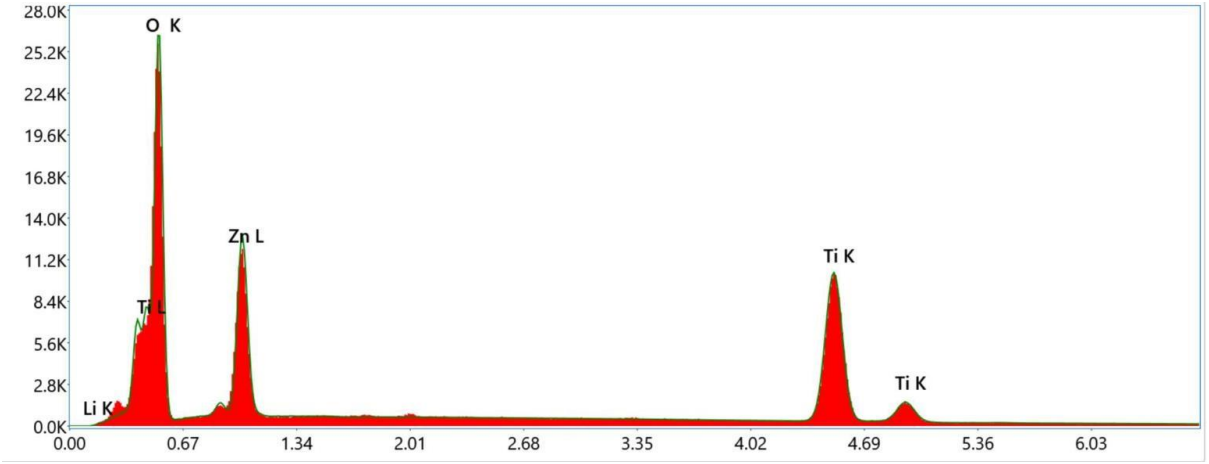


Fig. 11: EDS Images LZTO (Air)



(A)



(B)

Fig. 12: (A) & (B) EDS Map Sum Spectrum (Air) and (Argon) respectively

4.2 Electrochemical Analysis:

4.2.1 EIS Analysis:

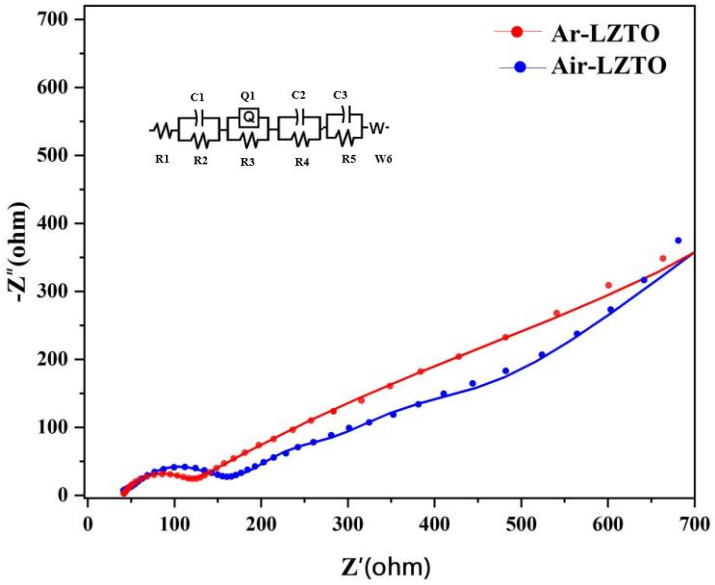


Fig. 13: Nyquist plot showing impedance of LZTO electrode

Electrochemical Impedance Spectroscopy (EIS) is a powerful analytical technique used to probe the kinetics, mass transport, and interfacial properties of electrochemical systems. In the Fig.4(a), the Nyquist Plot of Air-LZTO and Ar-LZTO is shown. In the plot, at high frequency Region, Both the Curve starts from the almost same point signifying electrolyte resistance signified by R1. First Depressed Semicircle is observed in both the samples with Ar-LZTO having smaller radii than Air-LZTO signifying lower Charge Transfer resistance in Ar-LZTO sample. The Diffusion coefficient of the both samples were calculated using following equation:

$$D_{Li^+} = \frac{0.5\,R^2T^2}{A^2n^2F^2C^2{\sigma_\omega}^2}$$

Where D_{Li^+},T, R, n, A, C, F and σ_ω represents Lithium-ion diffusion coefficient(cm^2s^{-1}), Temperature(K), Boltzmann constant (8.314 $Jmol^{-1}K^{-1}$), no. of electronics, area of electrode(cm^2),

Concentration of lithium ion (mole cm^{-3}), Faraday constant(F) and Warburg factor. The Li^+ diffusion coefficient of Argon and Air 2.57×10^{-15} and 1.93×10^{-15} respectively.

Further, there might be possibility of poorly separated semicircles which might be difficult to interpret using Conventional Circuit Modelling. Therefore, DRT (Distribution of Relaxation Time) approach is employed here to deconvolute individual relaxation process happening in the cell. DRT Method has been proven to be promising method for EIS analysis eliminating the limitation of Conventional Circuit Fitting Model. This Technique changes the Frequency-Domain Impedance Data to the Time-domain using the following equation :

$$Z(f) = R_{ohmic} + \int_0^{\infty} \frac{g(\tau)}{1 + j2\pi f\tau}\, d\tau$$

where f represents EIS frequency, $R_{(ohmic)}$ is the ohmic resistance corresponding to an impedance as the frequency approaches infinity, and g(τ) is the relaxation distribution function with a time constant (τ). This provides us the Well-Resolved peaks at different relaxation time where each peaks corresponds to distinguished relaxation process.

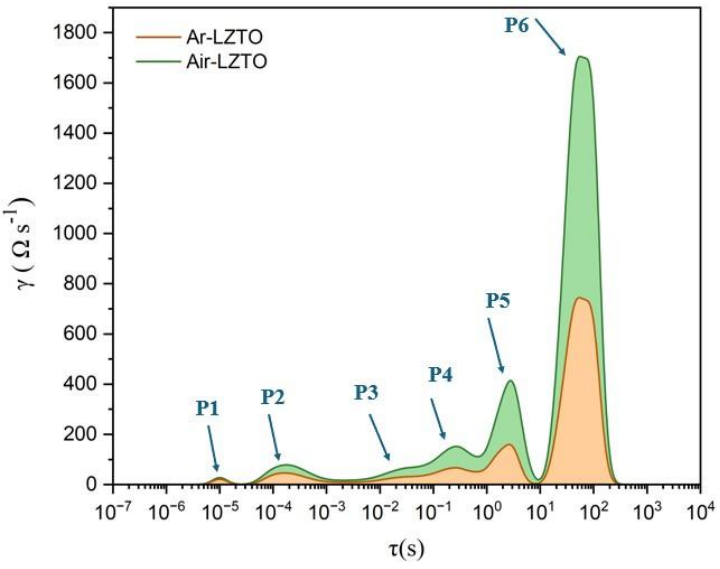


Fig. 14: Typical DRT profile of a Li-ion cell and the criteria used to evaluate DRT peaks

Fig. 14 shows the DRT Spectra of Air-LZTO and Ar-LZTO over the time-range of 10^{-7} to 10^{-3} resolves 6 distinct peaks where each peak corresponds to characteristic relaxation process. The First Relaxation peak P1 observed around 10^{-5}s corresponds to the Ohmic Resistance which represents the combination of contacts, electrolyte, and separator. Both the sample exhibits similar Peak, which suggests the same electrolyte resistance. The Second Peak P2 observed around 10^{-4}s corresponds to the Resistance arising from Solid Electrolyte interphase. The small peak of P2 of Ar-LZTO in comparison to Air-LZTO suggests the development of a less thick and more conductive SEI indicating less resistance to lithium- ion transport across SEI layer. The third peak P3 observed around 10^{-2}s corresponds to Charge Transfer Resistance. There is reduced peak observed in Ar-LZTO comparison to Air-LZTO indicating possibility of faster-charge kinetics. the fourth peak P4 observed around 10^{0} corresponds to Grain-Boundary Resistance. It represents interfacial resistance at grain boundary of the electrolyte, fifth peak observed around P5 represents Bulk-Ion Transfer Resistance. The decreased peak could correspond to enhanced conductivity of Ar-LZTO in comparison to Air-LZTO and Sixth Peak P6 represents Diffusion Resistance(Warburg Resistance). The reduced Ar-LZTO peak in comparison to Air-LZTO indicates improved lithium-ion diffusion kinetics and lower concentrations polarization. This might enhance rate capability and cycling stability of the material.

The area under the curve of the peak in DRT Spectrum represents Resistance corresponding to particular relaxation process. Table 2 shows resistance contribution of individual peak for Ar-LZTO and Air-LZTO. From the observation, It is clearly visible that Overall resistance contribution in Ar-LZTO is less than Air-LZTO signifying low resistance path and better Li^{+} ion diffusion kinetics [42].

Peaks	Ar-LZTO	Air- LZTO
P1(Ω)	1.80042E-4	5.24605E-5
P2(Ω)	0.02421	0.02945
P3(Ω)	0.23935	0.30652
P4(Ω)	9.07866	13.75258
P5(Ω)	297.16848	670.34555
P6(Ω)	82277.4676	2223.5884

Table 4: Resistance contribution of Electrochemical Process

4.1.1 Cyclic voltammetry:

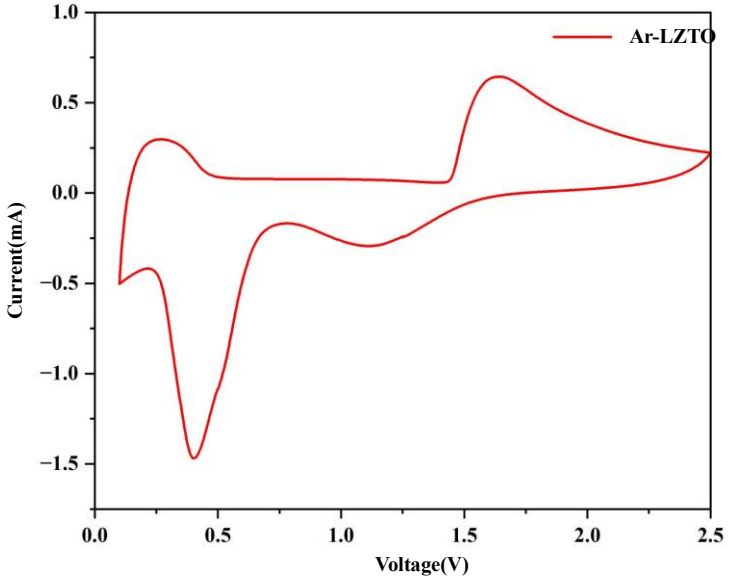


Fig.15: Cyclic voltammetry curves of synthesized Ar-LZTO

Figure shows the CV curve for third cycle of Ar-LZTO measured between 0.1 to 2.5V. The Cathodic and Anodic peak of Ar-LZTO was observed in this range corresponds 1.0V to

2.0V. The peaks in this range corresponds to Ti^{4+}/Ti^{3+} oxidation reaction during lithiation and de-lithiation process. However, there is reduction peak observed in 0.4-0.5V range corresponds to Ti^{4+} multiple restoration. By the help of Area under the curve we have calculated the value of specific capacity that's 198.4 mAh g^{-1} which is better than reported Air-LZTO.

CHAPTER 5

CONCLUSION & FUTURE SCOPE

5.1. Conclusion

A solid-state reaction method was used to synthesize LZTO in different environment. The XRD results revealed that prepared sample crystallizes in a cubic structure of Fd3m space group, and it matches perfectly with the standard database file no. JCPDS 086-1552. The average crystallite size was determined by Scherrer's equation was found to be ~29.88 nm (Ar- LZTO) and ~56.70 nm (Air-LZTO). The SEM of both the sample appear clustered together and The particle size evaluated with SEM was found to be ~180 nm and ~154.7 nm of LZTO-Air and LZTO-Ar respectively. The lithium-ion diffusion coefficient for the half-cell, as determined by EIS ranged from $2.57\times10^{-15}cm^2s^{-1}$ and $1.93\times10^{-15}cm^2s^{-1}$ of (Ar-LZTO) and (Air-LZTO) respectively, and the values of warburg factor are 78.87 $\Omega\ s^{-1/2}$ and 91.00 $\Omega\ s^{-1/2}$ of (Ar-LZTO) and (Air-LZTO) respectively. The value of specific capacity is around 198.4 $mAhg^{-1}$.

5.2. Future Scope:

The detailed electrochemical study of $Li_2ZnTi_3O_8$ (LZTO) will be carried out in the future to get a better insight into its lithium storage behavior. The specific capacity, rate capability, coulombic efficiency and cycling stability of the material will be systematically tested using galvanostatic charge–discharge (GCD) and long-term cycling tests. In addition, appropriate doping will be investigated to increase the electronic conductivity, structural stability, and lithium-storage capacity of LZTO. The studies it is hoped will yield valuable information in the design and development of high-performance LZTO anode materials for next generation lithium-ion batteries.

CHAPTER 6

REFERENCES

1. Liang, Y., Zhao, C. Z., Yuan, H., Chen, Y., Zhang, W., Huang, J. Q., ... & Zhang, Q. (2019). **A review of rechargeable batteries for portable electronic devices.** InfoMat, 1(1), 6-32.
2. ichtner, M., Edström, K., Ayerbe, E., Berecibar, M., Bhowmik, A., Castelli, I. E., ... & Weil, M. (2022). **Rechargeable batteries of the future—the state of the art from a BATTERY 2030+ perspective. Advanced Energy Materials**, 12(17), 2102904.
3. Bode, H. **Lead Acid Batteries,** 1977,(Brodd, RJ and Kordesch, KV Trans.).
4. Deng, D. **Li-ion batteries: basics, progress, and challenges, Energy Sci. Eng.** 3 (2015) 385–418.
5. Notten, P. H., & Danilov, D. L. (2014). Battery modeling: **A versatile tool to design advanced battery management systems. Advances in Chemical Engineering and Science,** 4(1), 62-72.
6. eyaseelan, C., Jain, A., Khurana, P., Kumar, D., & Thatai, S. (2020). **Ni-Cd Batteries. Rechargeable Batteries: History, Progress, and Applications,** 177-194.
7. Zou, C., Zhang, L., Hu, X., Wang, Z., Wik, T., & Pecht, M. (2018). **A review of fractional-order techniques applied to lithium-ion batteries, lead-acid batteries, and supercapacitors.** Journal of Power Sources, 390, 286-296.
8. McDowall, J. (1999, January). **Nickel-cadmium batteries for energy storage applications. In Fourteenth Annual Battery Conference on Applications and Advances**. Proceedings of the Conference (Cat. No. 99TH8371) (pp. 303-308). IEEE.
9. Taniguchi, A., Fujioka, N., Ikoma, M., & Ohta, A. (2001). **Development of nickel/metal-hydride batteries for EVs and HEVs. Journal of power sources,** 100(1-2), 117-124.
10. Arun, V., Kannan, R., Ramesh, S., Vijayakumar, M., Raghavendran, P. S., Siva Ramkumar, M., ... & Sundramurthy, V. P. (2022). **Review on li-ion battery vs nickel metal hydride battery in EV. Advances in Materials Science and Engineering**, 2022(1), 7910072.
11. Goodenough, J. B., & Park, K. S. (2013). **The Li-ion rechargeable battery: a perspective. Journal of the American Chemical Society**, 135(4), 1167-1176.

12. ONATOYINBO, O. (2021). **Cathode materials for lithium-ion batteries: a brief review. Journal of New Materials for Electrochemical Systems.**

13. Yao, J., Li, Y., Massé, R. C., Uchaker, E., & Cao, G. (2018). **Revitalized interest in vanadium pentoxide as cathode material for lithium-ion batteries and beyond. Energy Storage Materials,** 11, 205-259.
14. Cui, Z., Xie, Q., & Manthiram, A. (2021)**. A cobalt-and manganese-free high-nickel layered oxide cathode for long-life, safer lithium-ion batteries. Advanced Energy Materials**, 11(41), 2102421.
15. Julien, C. M., Zhang, X., & Mauger, A. (2017). **Lithium Iron phosphate: olivine material for high power Li-ion batteries.** Res Dev Mater Sci, 2, 3-6.
16. Huang, Y., Dong, Y., Li, S., Lee, J., Wang, C., Zhu, Z., ... & Li, J. (2021). **Lithium manganese spinel cathodes for lithium-ion batteries. Advanced Energy Materials**, 11(2), 2000997.
17. Prajapati, A. K., & Bhatnagar, A. (2023). **A review on anode materials for lithium/sodium-ion batteries. Journal of Energy Chemistry**, 83, 509-540.
18. Chen, S., Liu, C., Feng, R., Chen, Z., Lu, Y., Chen, L., ... & Wu, F. (2025). **Natural graphite anode for advanced lithium-ion Batteries: Challenges, Progress, and Perspectives**. Chemical Engineering Journal, 503, 158116.
19. Khan, M., Yan, S., Ali, M., Mahmood, F., Zheng, Y., Li, G., ... & Wang, Y. (2024). **Innovative solutions for high-performance silicon anodes in lithium-ion batteries: overcoming challenges and real-world applications.** Nano-micro letters, 16(1), 179.
20. Julien, C. M., & Mauger, A. (2024). **Fabrication of $Li_4Ti_5O_{12}$ (LTO) as anode material for Li-Ion batteries**. Micromachines, 15(3), 310.
21. Etuk, N. N., Popoola, A. P. I., Popoola, O. M., Uyor, U. O., & Ogbonna, V. E. (2025). **Review of SiO2-Based Composite Anode Electrode Materials for High-Energy Storage Lithium-Ion Batteries: Challenges and Recommendations for Future Development. Journal of Electronic Materials**, 54(6), 4241-4274.
22. Kainat, S., Anwer, J., Hamid, A., Gull, N., & Khan, S. M. (2024). **Electrolytes in lithium-ion batteries: advancements in the era of twenties (2020's). Materials Chemistry and Physics,** 313, 128796.
23. Korthauer, R. (Ed.). (2018). **Lithium-ion batteries: basics and applications**. Springer.
24. Colclasure, A. M., & Kee, R. J. (2010). **Thermodynamically consistent modeling of elementary electrochemistry in lithium-ion batteries. Electrochemica Acta,** 55(28),

8960-8973.

25. Zhao, L., Ding, B., Qin, X. Y., Wang, Z., Lv, W., He, Y. B., ... & Kang, F. (2022). **Revisiting the roles of natural graphite in ongoing lithium-ion batteries.** Advanced Materials, 34(18), 2106704.
26. Gulbinska, M. K.: **Lithium-ion battery materials and engineering: current topics and problems from the manufacturing perspective**. Springer (2014).
27. Gao, J., Shi, S. Q., & Li, H. (2016). **Brief overview of electrochemical potential in lithium- ion batteries**. Chinese Physics B, 25(1), 018210.
28. Zheng, G., Yang, Y., Cha, J. J., Hong, S. S., & Cui, Y. (2011). **Hollow carbon nanofiber-encapsulated sulfur cathodes for high specific capacity rechargeable lithium batteries.** Nano letters, 11(10), 4462-4467.
29. Lee, H., Yang, S., Kim, S., Song, J., Park, J., Doh, C. H., ... & Lee, Y. M. (2022). **Understanding the effects of diffusion coefficient and exchange current density on the electrochemical model of lithium-ion batteries.** Current Opinion in Electrochemistry, 34, 100986.
30. Yu, P., Popov, B. N., Ritter, J. A., & White, R. E. (1999). **Determination of the lithium-ion diffusion coefficient in graphite**. Journal of The Electrochemical Society, 146(1), 8-14.
31. Nzereogu, P. U., Omah, A. D., Ezema, F. I., Iwuoha, E. I., & Nwanya, A. C. (2022). **Anode materials for lithium-ion batteries**: A review. Applied Surface Science Advances, 9, 100233.
32. Chang, H.; Wu, Y. R.; Han, X.; Yi, T. F. **Recent developments in advanced anode materials for lithium-ion batteries**. *Energy Mater.* **2021**, *1*, 100003. http://dx.doi.org/10.20517/energymater.2021.02
33. Prajapati, A. K., & Bhatnagar, A. (2023). **A review on anode materials for lithium/sodium-ion batteries.** *Journal of Energy Chemistry*, *83*, 509-540.
34. Yu, S. H., Feng, X., Zhang, N., Seok, J., & Abruña, H. D. (2018). **Understanding conversion-type electrodes for lithium rechargeable batteries**. *Accounts of chemical research*, *51*(2), 273-281.
35. Fang, S., Bresser, D., & Passerini, S. (2022). **Transition metal oxide anodes for electrochemical energy storage in lithium-and sodium-ion batteries**. *Transition metal oxides for electrochemical energy storage*, 55-99.

36. Park, H., Kim, K., Jeong, K., Kang, J. S., Cho, H. H., Thirumalraj, B., Sung, Y.E., Han, H.N., Kim, J.H., Dunand, DC., and Choe, H.: **Integrated porous cobalt oxide/cobalt anode with micro-and nano-pores for lithium- ion battery.** Applied Surface Science, 525, 146592, (2020).
37. Khalil, A., Lalia, B. S., and Hashaikeh, R.: **Nickel oxide nanocrystals as a lithium-ion battery anode: structure-performance relationship**. Journal of Materials Science, 51, 6624-6638 (2016).
38. Lv, L., Peng, M., Wu, L., Dong, Y., You, G., Duan, Y., Yang, W., He, L., and Liu, X.: **Progress in iron oxides-based nanostructures for applications in energy storage.** Nanoscale Research Letters, 16(1), 138, (2021)
39. Rajagopalan, K., Ramasubramanian, B., Velusamy, S., Ramakrishna, S., Kannan, A. M., Kaliyannan, M., & Kulandaivel, S.: **Examining the economic and energy aspects of manganese oxide in Li-ion batteries.** Materials Circular Economy, 4(1), 22, (2022).
40. Zhao, Y., Li, X., Yan, B., Xiong, D., Li, D., Lawes, S., & Sun, X. (2016). **Recent developments and understanding of novel mixed transition-metal oxides as anodes in lithium-ion batteries.** *Advanced Energy Materials*, *6*(8), 1502175.
41. Chen, Z., Wang, T., Liu, M., Duan, P., Xiong, F., Zhou, Y., ... & Li, C. (2023). **Polycrystal Li2ZnTi3O8/C anode with lotus seedpod structure for high-performance lithium storage**. *Frontiers in Chemistry*, *11*, 1135325.
42. Iurilli, P., Brivio, C., & Wood, V. (2022). **Detection of lithium-ion cells' degradation through deconvolution of electrochemical impedance spectroscopy with distribution of relaxation time**. *Energy Technology*, *10*(10), 2200547.